Short- to Medium-Range Atomic Order and Crystallite Size of the Initial FeS Precipitate from Pair Distribution Function Analysis

F. M. Michel,*,† S. M. Antao,† P. J. Chupas,‡ P. L. Lee,‡ J. B. Parise,† and M. A. A. Schoonen†

Center for Environmental Molecular Science (CEMS), Department of Geosciences, Stony Brook University, Stony Brook, New York 11794, and XOR, Advanced Photon Source, Argonne National Laboratory, Argonne, Illinois 60439

Received April 26, 2005. Revised Manuscript Received October 3, 2005

Pair distribution function analysis (PDF) of X-ray diffraction data, collected at 11-IDC and 1-ID at the Advanced Photon Source, provides the atomic structure and primary crystallite size of FeS both freshly precipitated (FeS_{fresh}) and aged (FeS_{aged}). The short- to medium-range structure of both FeS_{fresh} and FeS_{aged} are nearly identical with that of highly crystalline (bulk) mackinawite. Attenuation in the observed range of structural coherence of the PDF for FeS_{fresh} indicates an average crystallite size on the order of ∼2 nm. This range of structural coherence increased with aging of the sample under hydrothermal conditions due to growth of the individual crystallites, although the mechanism by which this growth occurs is not clear at present. Electron microscopic imaging confirms the presence of individual nanoscale crystallites and provides some insight into their aggregation behavior as larger clusters. The initial, fresh precipitate does not exhibit long-range atomic structure because it is nanocrystalline. The so-called X-ray amorphous nature of FeS_{fresh} is the result of the limited range of structural coherence imposed by the size of the individual crystallites rather than the result of a lack of medium- and long-range atomic order. We propose that the discrepancies in the literature over crystallite size and the atomic structure of FeS_{fresh} are due primarily to the varying degrees of aggregation of uniformly distributed and nanocrystalline FeS particles.

Introduction

The properties of the Fe−S system are of major interest and importance in environmental, geological, and planetary science. In the Earth's crust, pyrite (FeS_2) formation from so-called disordered or amorphous FeS is a key process in several geochemical cycles.[1] FeS is environmentally significant in the sequestration and remobilization of heavy metal contaminants such as Cu, Cd,[2] As,[3] Ni, and Co[4] and has recently been shown to react with contaminants such as dissolved $Cr^{(VI)}$ species.[5] FeS is also an important product during diagenesis in marine sediments. Hydrogen sulfide, produced by sulfate-reducing bacteria, reacts with iron sources within the sediments to form FeS.[6,7] The first step in the formation of iron sulfides under aqueous conditions is the nucleation of a reduced, short-range-ordered iron monosulfide (FeS_{fresh}) that is generally believed to be a precursor to crystalline (bulk) mackinawite.[8] Subsequently, mackinawite itself serves as a precursor to the stable Fe−S phase, pyrite. A structure model for the initial FeS precipitate is required as a first step to studying the consequences of its formation, transformation and reactivity under varying conditions as well as the sequestration of contaminants. Until this study, the short- to medium-range crystal structure and primary crystallite size of the initial FeS precipitate, often referred to in the earth science literature as amorphous FeS, had not yet been resolved.

Research Strategy

FeS was formed in this study by the reaction of ferrous iron with sulfide in aqueous solution at room temperature (22 ± 2 °C). The initial precipitate formed by mixing the iron and sulfide solutions will hereafter be referred to as freshly precipitated FeS or simply FeS_{fresh}. The precipitation reaction was conducted at pH values varying between ∼5 and ∼9. Both wet and dry samples of the FeS_{fresh} as well as an aged precipitate (hereafter referred to as FeS_{aged}) were examined. Due to an absence of well-defined Bragg reflections in FeS_{fresh} and FeS_{aged}, atomic pair distribution function (PDF) analysis was used as a structural probe. This technique, originally developed to investigate the short- to medium-range atomic order in liquids and glassy materials, has been described in detail elsewhere.[9,10] In short, the PDF enables the gathering of three important pieces of information about pairs of atoms in the structure of interest: the peak position

* Corresponding author e-mail: fmichel@ic.sunysb.edu.
† Stony Brook University.
‡ Argonne National Laboratory.

(1) Wilkin, R. T.; Barnes, H. L. *Geochim. Cosmochim. Acta* **1996**, *60*, 4167−4179.
(2) Parkman, R. H.; Charnock, J. M.; Bryan, N. D.; Livens, F. R.; Vaughan, D. J. *Am. Mineral.* **1999**, *84*, 407−419.
(3) Wolthers, M. Geochemistry and environmental mineralogy of the iron−sulphur−arsenic system. Ph.D. Thesis, Utrecht, 2003.
(4) Morse, J. W.; Millero, F. J.; Cornwell, J. C.; Rickard, D. *Earth-Sci. Rev.* **1987**, *24*, 1−42.
(5) Mullet, M.; Boursiquot, S.; Ehrhardt, J. *Colloids Surf. A* **2004**, *244*, 77−85.
(6) Berner, R. A. *Am. J. Sci.* **1970**, *268*, 1−23.
(7) Donald, R.; Southam, G. *Geochim. Cosmochim. Acta* **1999**, *63*, 2019−2023.
(8) Schoonen, M. A. A.; Barnes, H. L. *Geochim. Cosmochim. Acta* **1991**, *55*, 1505−1514.

10.1021/cm050886b CCC: $30.25
Published on Web 11/16/2005

indicating the average distance separating the pair, the integrated intensity of each peak yielding number of coordinated atoms, and the width and shape of the peak indicating the static and/or dynamic disorder in the pair. Additionally, the range of the PDF indicates the size of coherently scattering structural domains and therefore, in certain cases, provides a means for determining average primary crystallite sizes.[11−14] As it has been historically described as an X-ray amorphous material,[15−17] the scattering from FeS_{fresh} was presumed to be generally weak, especially if in the presence of an aqueous solution. Therefore, a requirement of the study was to collect data of sufficient quality across a wide range of momentum transfer (Q) to obtain a properly normalized total scattering structure function $S(Q)$ and pair distribution function $G(r)$. The purpose was to go beyond fingerprinting, by comparing diffraction patterns, to deriving testable structure models by fitting the real-space $G(r)$ derived from the scattering data. Without properly normalized $S(Q)$, this refinement of competing models is not possible. A sufficient range of $S(Q)$ requires use of intense, monochromatic, high energy X-rays available at the Advanced Photon Source (APS), a third generation synchrotron source.

Experimental Methods

Chemicals. $Fe(NH_4)_2(SO_4)_2 \cdot 6H_2O$ (Mohr's salt) (99.4%), $Na_2S \cdot 9H_2O$ (NaSH/NaOH or sulfide) (99%), HCl (certified A.C.S. Plus), and CH_3COOH (acetic acid) were from Fisher Chemicals; $C_8H_5O_4K$ (potassium hydrogen phthalate) (+99.5%) was from Aldrich; KCl (+99%) and NaOH (pellets) (98.8%) were from J. T. Baker; iron wool (super fine 0000) was from Rhodes American. Buffer solutions of pH 4 were prepared by the addition of 50 mL of 0.1 M potassium hydrogen phthalate to 0.1 mL of 0.1 M HCl. Buffer solutions of pH 12 were prepared by the addition of 25 mL of 0.2 M KCl to 6 mL of 0.2 M NaOH. All of the chemicals were analytical grade and were used as received without additional purification. All solutions were prepared using water that was deionized (EasyPure, filtered 0.2 μm, UV/UF) and purged with N_2 (99.99% pure) for at least 30 min to remove dissolved molecular oxygen.[18] All solutions were prepared at room temperature (22 ± 2 °C) in an anaerobic glovebox purged with a mixture of N_2 (97%) and H_2 (3%) and equipped with a CoyLabs oxygen removal system and digital O_2 and H_2 analyzer/indicator. Sample FeS-E was an exception and is described below.

Syntheses. All FeS samples (except FeS-Bulk) were synthesized by direct injection of 0.3 M ferrous ammonium sulfate solution (Mohr's salt) into 0.3 M sulfide (NaSH/NaOH) solution with a ratio of approximately 1:1. This common method of precipitating so-called amorphous FeS from solution was described initially by Rickard.[19] In some cases, a pH 4 or pH 12 buffer solution was added to the sulfide solution prior to the addition of the Mohr's salt solution to lower or increase, respectively, the pH at the time of precipitation.[8] Highly crystalline (bulk) FeS was synthesized according to the method described by Lennie et al.[28] and involved the reaction of metallic iron and sulfide. It is important to note that great care was taken to minimize the potential for oxidation of the synthetic FeS by exposure to atmospheric oxygen. All syntheses were carried out at room temperature (22 ± 2 °C) and in a glovebox (excluding FeS-E) under a completely anoxic H_2-N_2 atmosphere. The anoxic H_2-N_2 atmosphere in the chamber was maintained using a Pd-catalyst and monitored continuously with a dedicated, real-time oxygen/hydrogen sensor. Sample identification and an overview of synthesis conditions are outlined in Table 1.

Table 1. Sample Identification and Synthesis Conditions[a]

manu sample ID	reagent volumes (mL): Mohr's salt	sulfide	buffer (pH)	pH	aged (Y/N)	dried (Y/N)
FeS-A	10	10	10 (4)	5.3	N	Y
FeS-B	10	10	5 (4)	7.2	N	Y
FeS-C	10	10		8.0	N	Y
FeS-D	10	10	2.5 (12)	8.2	N	Y
FeS-E	15	17	10 (4)	5.5	N	N
FeS-F	500	525		9.2	Y	Y

manu sample ID	reagent volumes (mL): iron wool	sulfide	acetic acid/ acetate	pH	aged (Y/N)	dried (Y/N)
FeS-Bulk	5 g	100 mL	500 mL	1.7−4.5	N	Y

[a] Ferrous ammonium sulfate hexahydrate (Mohr's salt) was used as the source of Fe^{2+} for FeS-A through FeS-F. Samples FeS-A through FeS-E were synthesized using 0.3 M stock solutions. FeS-F was synthesized using 0.2 M stock solutions and was aged for 1 week at 70 °C as part of a large batch of sample. FeS-Bulk was synthesized according to the prep of Lennie et al.[28].

Fresh Precipitates: *Dry* (*FeS-A*$_{(pH\ 5.3)}$, *FeS-B*$_{(pH\ 7.2)}$, *FeS-C*$_{(pH\ 8.0)}$, *and FeS-D*$_{(pH\ 8.2)}$). Samples FeS-A through FeS-D were synthesized and processed according to the protocol outlined in Table 2. Upon mixing, the precipitated solid phase and supernatant solution were sealed in 50 mL plastic centrifuge tubes under anoxic conditions in preparation for rinsing of the solid phase. The precipitates were dried in the anaerobic glovebox within less than 2 h from the time of mixing.

Fresh Precipitate: *Wet* (*FeS-E*$_{(pH\ 5.5)}$). Sample FeS-E was synthesized at the APS and analyzed within about 8 h after the time of mixing the reagents. The protocol was similar to that used for the dry precipitates but with several differences outlined in Table 3. The reagents were mixed in a fume hood under flowing N_2 because a glovebox was not available for use. The sample was centrifuged for one cycle (5 min at 3000 rpm) in a 50 mL centrifuge tube. The resulting supernatant was then removed leaving the dense, wet FeS slurry that was packed into a 3 mm polyimide capillary and capped on both ends with wax under a stream of N_2. The loaded capillary was then centrifuged a second time to squeeze out more of the supernatant solution leaving a denser sample for analysis. This sample was analyzed to evaluate the effects of water on the structure, specifically to assess the degree of lattice relaxation relative to a dry sample precipitated under similar pH conditions (FeS-A).

Aged Precipitate (*FeS-F*$_{(pH9.2)}$). FeS-F was synthesized following generally the same protocol as samples A−D but in addition was

(9) Egami, T. *J. Phys. Chem. Solids* **1994**, *56*, 1407−1413.
(10) Egami, T.; Billenge, S. J. L. *Underneath the Bragg Peaks: Structural Analysis of Complex Materials*; Elsevier: Oxford, 2003.
(11) Billenge, S. J. L.; Petkov, V.; Proffen, T. *Commission on Powder Diffraction of the International Union of Crystallography Newsletter*; 2000.
(12) Hall, B. D.; Zanchet, D.; Ugarte, D. *J. Appl. Crystallogr.* **2000**, *33*, 1335−1341.
(13) Page, K.; Proffen, T.; Terrones, H.; Terrones, M.; Lee, L.; Yang, Y.; Stemmer, S.; Seshadri, R.; Cheetham, A. K. *Chem. Phys. Lett.* **2004**, *393*, 385−388.
(14) Neder, R. B.; Korsunskiy, V. I. *J. Phys.*: *Condens. Matter* **2005**, *17*, S125−S134.
(15) Berner, R. A. *Am. J. Sci.* **1967**, *265*, 773−785.
(16) Rickard, D. *Chem Geol.* **1989**, *78*, 315−324.
(17) Herbert, R. B.; Benner, S. G.; Pratt, A. R.; Blowes, D. W. *Chem. Geol.* **1998**, *144*, 87−97.
(18) Butler, I. B.; Schoonen, M. A. A.; Rickard, D. F. *Talanta* **1994**, *41*, 211−215.
(19) Rickard, D. *Stockholm Cont. Geol.* **1969**, *20*, 67−95.

Table 2. Protocol for Sample Preparation (FeS-A, -B, -C, -D, and -F)[a]

step	action
synthesis	**mix reagents and precipitate FeS_{fresh} in 50 mL centrifuge tubes (followed by aging for 1 week at 70 °C in the case of FeS-F)**
	sonicate (1 min) and vortex (20 s)
	centrifuge 3 min at 5000 rpm
	decant supernatant 1 and add ~45 mL of 1 mM sulfide solution
rinse cycle 1	centrifuge 5 min at 5000 rpm
	decant supernatant and add ~45 mL of 1 mM sulfide solution
	sonicate (1 min) and vortex (20 s)
rinse cycle 2	repeat cycle 1
rinse cycle 3	centrifuge 5 min at 5000 rpm
	decant supernatant (including colloidal suspension[b])
extraction	**filter solid-phase product**
	dry product under N_2 stream
	lightly grind using agate mortar and pestle
loading	**powders loaded into 1 mm polyimide capillaries and capped with glass wool and an amorphous silicone vacuum grease**
storage	**loaded capillaries were sealed in individual glass culture tubes pending transport to APS**

[a] Boldface type indicates that the actions were carried out in glovebox under completely anoxic conditions. Regular type indicates that the actions were carried out on a sample sealed in a centrifuge tube and capped with the H_2-N_2 mix. [b] Supernatant included a stable suspension of colloidal FeS particles and was preserved for TEM imaging.

Table 3. Protocol for Sample Preparation (FeS-E)[a]

step	action
synthesis	**mix reagents and precipitate FeS in 50 mL centrifuge tubes**
	centrifuge 5 min at 3000 rpm
	decant supernatant and add ~45 mL of 1 mM sulfide solution
rinse cycle 1	centrifuge 5 min at 3000 rpm
	decant supernatant
loading	**wet slurry loaded into 3 mm polyimide capillaries and capped with wax**
centrifuge	loaded capillaries were placed in 15 mL centrifuge tubes and centrifuged for 5 min at 3000 rpm

[a] Boldface type indicates that the actions were carried out under a stream of N_2.

aged for one week at elevated temperature in a water bath as part of a large sample batch. FeS-F was formed by the direct injection of 500 mL of 0.2 M Mohr's Salt into 525 mL of 0.2 M sulfide solution. The resultant product and supernatant were sealed under anoxic conditions in a 1 L glass vessel and immersed in a preheated 70 °C water bath for 1 week. The sample was agitated periodically by gently shaking. At the end of 1 week of aging, a portion of the sample was then separated under anoxic conditions in preparation for processing and characterization as described below.

Crystalline FeS (*FeS-Bulk*). FeS-Bulk was synthesized according to the protocol described by Lennie et al.[28] In brief, finely divided iron wool was rinsed with laboratory grade acetone prior to immersion in a beaker containing 500 mL of a 0.5 M acetic acid/acetate buffer (pH 1.7) solution. After approximately 30 min, sufficient H_2 evolved from the reaction between the steel wool and acetic acid for the wool to be brought to the surface by trapped gas. Sulfide was subsequently added slowly to the solution and FeS spalled off of the surface of the iron and settled to the bottom of the beaker. The pH of the solution, initially at 1.7, increased to 4.5 when 100 mL of sulfide solution was added. The solution was allowed to sit for approximately 2 h before the supernatant was decanted. A stirring bar magnet was used to recover any remaining fragments of metallic iron from the settled FeS precipitate. The recovered solid phase FeS was then washed using the centrifuge-rinsing protocol described below and subsequently filtered and dried. Characterization of the solid phase FeS by XRD revealed the presence of a minor percentage of greigite formed as a secondary phase. Because the synthesis was carried out under completely anoxic conditions we speculate that greigite (Fe_3S_4) formed in this instance from oxidized (ferric) iron present as impurities in the iron wool.

Sample Preparation. *Centrifuge and Rinsing.* The solid-phase FeS precipitates (excluding FeS-E) were each rinsed three times using a protocol developed to minimize oxidation of the metal sulfide and yet to remove most of the electrolytes associated with the starting reagents. This rinsing protocol, summarized in Table 2, is a modified and expanded version of a protocol first described by Herbert et al.[20] In brief, during three cycles the FeS slurry was centrifuged for 5 min at 5000 rpm after which the loaded tubes were returned to the glovebox where most of the supernatant was removed from each and replaced by approximately 45 mL of 1 mM sulfide rinse solution. The sulfide rinse solution also served as a scavenger of oxygen preventing the surface oxidation of the FeS precipitate. The solid phase was then re-suspended in each fresh rinse solution using first a vortexer for 20 s followed by agitation in a sonicator bath for 1 min. This process was repeated and following the third and final centrifuge−rinse cycle the solid-phase FeS product was extracted under anoxic conditions.

Drying. The resulting wet FeS slurry was filtered over a membrane filter with 0.2 μm diameter pores. It was observed that the liquid fraction was removed very slowly because the pores of the membrane filter were quickly clogged by the solid-phase precipitate. The solid-phase collected on the filter was dried at room temperature in the glovebox under a stream of N_2.

Loading of Capillaries. Both dry and wet samples were pre-loaded into 1 mm or 3 mm o.d. polyimide (Kapton) capillaries under completely anoxic atmosphere and capped at both ends to inhibit gas exchange and oxidation. The loaded capillaries were then sealed under anoxic conditions (excluding FeS-E) in glass culture tubes with septum caps for transport to the APS. As described earlier, the FeS-E sample was prepared on-site at the APS.

Sample Characterization. Over 30 synthetic FeS samples were characterized at the APS. However, only data for seven representative samples are discussed in detail in this paper. Sample identification and the conditions under which they were analyzed are described in Tables 1−3. Data for the freshly precipitated samples that were analyzed as dry powders (FeS-A, -B, -C, and -D) and also the wet slurry (FeS-E) were collected at BESSRC−CAT 11-IDC. The aged precipitate (FeS-F) and highly crystalline sample (FeS-Bulk) were analyzed at XOR 1-ID.

High Energy Powder X-ray Diffraction (*XRD*) *at the Advanced Photon Source.* High energy powder XRD data was collected at 11-IDC (115 keV, $\lambda = 0.1076$ Å[21]) and at 1-ID (79.9 keV, $\lambda = 0.15513$ Å and 99.9 keV, $\lambda = 0.1240$ Å[22]). A CeO_2 standard (NIST diffraction intensity standard set: 674a) was used to calibrate the sample-to-detector distance and the tilt of the detector relative to the incident beam path. The energy calibration was initially achieved

(20) Herbert, R. B., Jr.; Benner, S. G.; Pratt, A. R.; Blowes, D. W. *Chem. Geol.* **1998**, *144*, 87−97.
(21) Rutt, U.; Beno, M. A.; Strempfer, J.; Jennings, G.; Kurtz, C.; Montano, P. A. *Nucl. Instr. Methods A* **2001**, *467−468*, 1026−1029.
(22) Shastri, S. D.; Fezzaa, K.; Mashayekhi, A.; Lee, W.-K.; Fernandez, P. B.; Lee, P. L. *J. Synchrotron Radiat.* **2002**, 317−322.

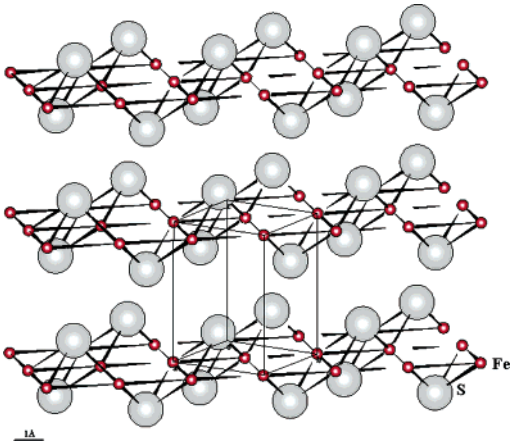

Figure 1. Layered structure of mackinawite. Small spheres represent Fe atoms; large spheres represent S atoms; a unit cell is outlined. Fe is tetrahedrally coordinated by S atoms and in square planar coordination with Fe.

using the gold absorption edge as reference and, if increased to higher energies (i.e., 99.9 or 115 keV), was recalibrated by refinement of the wavelength and fixing of the sample-to-detector distance. The radiation scattered by the calibrant and samples was collected on a MAR-345 image plate detector system and processed using the program Fit-2D.[23,24] A polarization correction was applied during integration of the data. Data were also collected on both blank (empty) polyimide capillaries (1 and 3 mm) and on those loaded with deionized water for background correction during PDF analysis. The sample capillary was rotated during data collection.

Pair Distribution Function (*PDF*) *Analysis.* The total scattering structure function $S(Q)$ and PDF $G(r)$ were obtained using PDFgetX2[25] where standard corrections were applied as well as those unique to image-plate geometry.[26] The structure of crystalline mackinawite consists of tetrahedral layers of Fe and S atoms (Figure 1). The Fourier transform of the normalized and scaled $S(Q)$ or $Q[S(Q) - 1]$ (Figure 2a−f), resulted in the PDF, or $G(r)$, which corresponds to real-space interatomic distances. The model for crystalline mackinawite was fitted to the experimental PDF, and the structural parameters of the model were refined and plotted using the programs PDFfit and Kuplot,[27] respectively (Figure 3a−f). The initial atomic coordinates, cell parameters, isotropic displacement parameters (U), and spacegroup ($P4/nmm$) were those of Lennie et al.[28] Two additional parameters δ and σ_Q were incorporated in each refinement to model sharpening of PDF near neighbor peaks due to correlated motion between atom pairs and the exponential decay of the PDF, respectively. If within the resolution of the instrument, the exponential decay of the PDF can be attributed to a limited range of structural coherence in nanocrystalline materials (i.e., primary crystallite size). In the case of highly crystalline samples, the decay of the PDF represents the resolution of the instrument.[13]

Transmission Electron Microscopy (*TEM*). Selected FeS samples were mounted directly from the stable suspensions captured during the centrifuge−rinse processing outlined in Table 2. Prior to mounting on grids, the pH of the suspension was adjusted down to ~4 using HCl in order to disaggregate the FeS clusters in solution

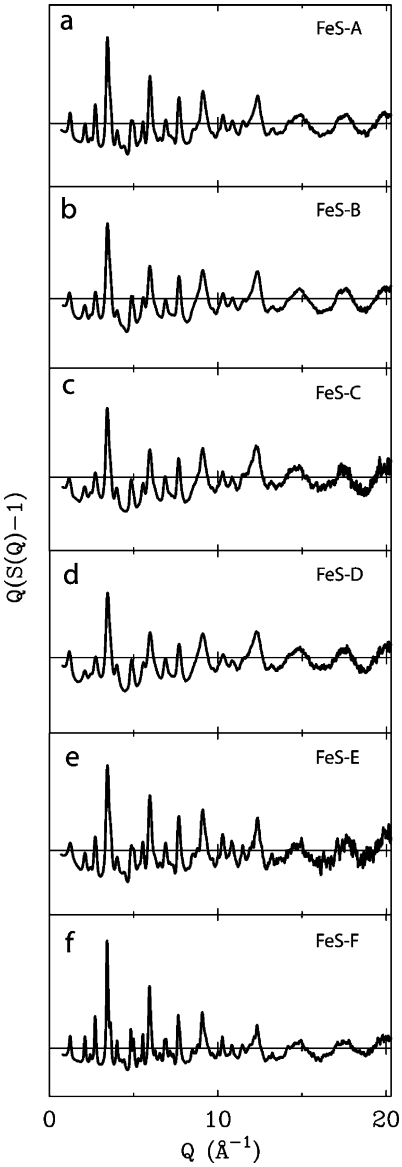

Figure 2. (a−f) Normalized scattering function $Q[S(Q) - 1]$ vs Q (Å^{-1}) for each of the six FeS samples.

(unpublished dynamic light scattering results). FeS particles in solution were transferred under completely anoxic conditions onto 300 mesh, 3 mm, and carbon-coated copper grids with Formvar. The mounted grids were dried under a stream of N_2 and then stored temporarily in glass vials and capped under anoxic conditions for transport to the TEM. The grids were each exposed to atmospheric oxygen for less than 1 min on average while being transferred from the N_2-capped vials to a beryllium TEM sample holder before being placed under high vacuum in the microscope. Imaging was performed using a Philips CM12 scanning TEM with a high brightness (LaB_6) electron gun.

Results

Structural analysis using the PDF method involves a comparison between PDFs generated from the experimental scattering data and a model PDF. In this study the model PDF was based on the structure of crystalline mackinawite[28] and was refined in real-space and fit to the experimental

(23) Hammersley, A. P. ESRF Internal Report ESRF98HA01T, 1998.
(24) Hammersley, A. P.; Svenson, S. O.; Hanfland, M.; Hauserman, D. *High-Pressure Res.* **1996**, *14*, 235−248.
(25) Qiu, X.; Thompson, J. W.; Billenge, S. J. L. *J. Appl. Crystallogr.* **2004**, *37*, 678.
(26) Chupas, P. J.; Qui, X.; Hanson, J. C.; Lee, P. L.; Grey, C. P.; Billinge, S. J. L. *J. Appl. Crystallogr.* **2003**, *36*, 1342−1347.
(27) Proffen, T.; Billenge, S. J. L. *J. Appl. Crystallogr.* **1999**, *32*, 572−575.
(28) Lennie, A. R.; Redfern, S. A. T.; Schofield, P. F.; Vaughan, D. J. *Mineral. Mag.* **1995**, *59*, 677.

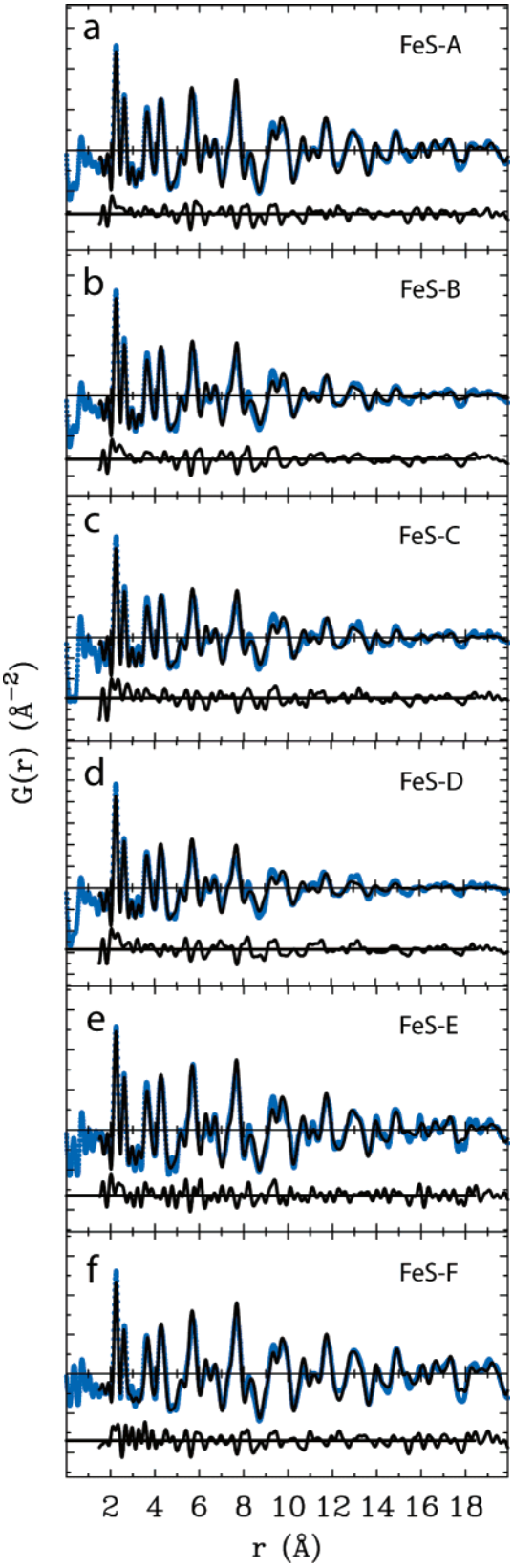

Figure 3. (a−f) $G(r)$ or the PDF vs distance is plotted with the experimental data (blue circles) fitted by the refined model PDF (solid black) shown. A difference plot is included beneath each data set as an indication of fit.

PDFs for each of the seven representative samples. The fits of the single-phase mackinawite model are included as Figure 3a−f. The PDF has peaks at characteristic distances separating pairs of atoms and thus, $G(r)$ is a measure of the probability of finding an atom at a distance r from a reference atom and so describes the atomic arrangement (structure) of materials.[10] Unit cell parameters, isotropic displacement parameters, atom positions (S z-position), resolution dampening (σ_Q), a peak sharpening factor (δ), and scale factor were all refined simultaneously using PDFFit (Tables 4 and 5). A "goodness of fit" indicator (R_w) is also reported for each refinement, and information regarding the acceptable ranges for R_w and accuracy of the technique have been discussed elsewhere.[29−31]

Unit Cell Parameters, Bond Lengths, and Angles. The cell parameters derived from PDF refinement of all of the FeS samples analyzed (Table 4) are in good agreement with those reported from Rietveld refinement of crystalline mackinawite[28] and with the highly crystalline sample (FeS-Bulk) analyzed here (Table 5). Bond lengths and angles calculated using PDFFit after each refinement are listed in Tables 6 and 7. The analysis of the structure of FeS_{fresh} and FeS_{aged} are nearly identical with previous reports on the structure of crystalline mackinawite.[28,32] A crystalline CeO_2 standard was also analyzed during each of the three data collection events and the results of the refinements are included for reference (Tables 4 and 5).

Structure Relaxation. The c-parameter corresponding to the atomic spacing between basal planes in the layered mackinawite structure of FeS_{fresh} and FeS_{aged} shows only minor relaxation (less than ∼1%) as compared to bulk FeS. Further, the refined a-parameter corresponding to Fe in square planar coordination is also very close to that of the bulk sample. As will be discussed, these refined values are not consistent with those reported in a recent investigation,[3] which concluded that a portion of the initial precipitate forms with a highly relaxed structure. The structure of the initial precipitate also did not change when dispersed in an aqueous media. The present study includes two samples (FeS-A and FeS-E) that were initially precipitated under similar pH conditions but differed in that sample FeS-E was analyzed as a dense wet slurry while FeS-A was in the form of a thoroughly dried sample. The refined model PDFs were fitted to the experimental PDFs (Tables 4 and 6) and no significant differences in lattice parameters were observed. This indicates that drying of the material does not result in any significant structural changes.

PDF Attenuation and Particle Size. The primary method of synthesis employed in this study involves a sudden generation of high supersaturation levels and results in the rapid nucleation of very small particles at the time of mixing.[33] As mentioned above, the PDF method has been demonstrated to be a useful tool in determining the primary crystallite size of nanocrystalline materials through an evaluation of the attenuation of the PDF resulting from a

(29) Toby, B. H.; Egami, T. *Acta Crystallogr. A* **1992**, *48*, 336−346.
(30) Petkov, V.; Billinge, S. J. L.; Larson, P.; Mahanti, S. D.; Vogt, T.; Rangan, K. K.; Kanatzidis, M. G. *Phys. Rev. B* **2002**, *65*.
(31) Petkov, V.; Billinge, S. J. L.; Heising, J.; Kanatzidis, M. G. *J. Am. Chem. Soc.* **2000**, *122*, 11571−11576.
(32) Lennie, A. R.; Vaughan, D. J.; Dyar, M. D. E.; McCammon, C. E.; Schaefer, M. W. E. *Spec. Publ.—Geochem. Soc.* **1996**, *5*, 117−131.
(33) Waychunas, G. A. In *Nanoparticles and the Environment*; Banfield, J. F., Navrotsky, A., Eds.; The Mineralogical Society of America: Washington, DC, 2001; Vol. 44, pp 105−162.

Table 4. Refinement Results[a]

parameter	FeS-A(1)[b]	FeS-B(1)	FeS-C(1)	FeS-D(1)	FeS-E(1)	FeS-F(2)	Rietveld parameters[b]	CeO_2(1)	CeO_2(2)
a (Å)	3.685(6)	3.687(2)	3.696(1)	3.694(6)	3.685(4)	3.695(1)	3.6735(4)	5.403(8)	5.419(9)
c (Å)	5.037(4)	5.082(9)	5.083(3)	5.089(3)	5.068(2)	5.057(6)	5.0328(7)		
S *z*-position	0.2550	0.2533(6)	0.2528(5)	0.2523(6)	0.2537(6)	0.2553(5)	0.2602(3)		
R_w (%)	24.9	30.4	34.1	33.6	28.0	27.2		15.4	17.5
σ_Q (Å^{-1})	0.094(8)	0.133(8)	0.123(6)	0.146(1)	0.098(2)	0.077(8)		0.059(2)	0.032(8)
δ	0.090(3)	0.097(4)	0.100(5)	0.100(8)	0.090(7)	0.082(8)		0.093(7)	0.053(6)
U_{Fe} (Å^2)	0.009(7)	0.009(9)	0.010(2)	0.010(5)	0.009(6)	0.009(9)		0.005(6)	0.004(5)
U_S (Å^2)	0.009(7)	0.010(1)	0.009(6)	0.010(2)	0.009(9)	0.009(7)		0.023(4)	0.023(7)
pH	5.3	7.2	8	8.2	5.5	9.2			
aging	none	none	none	none	none	1 week at 70 °C			

[a] U = isotropic displacement parameter. (1) indicates data collected at 11-IDC (energy = 115 keV). (2) indicates data collected at 1-ID (energy = 99.9 keV). [b] Cell parameters reported by Lennie et al.[28] for a Rietveld refinement of crystalline mackinawite.

Table 5. Refinement Results (FeS-Bulk)[a]

parameter	FeS-Bulk(3)	Rietveld parameters[b]	CeO_2(3)
a (Å)	3.676(6)	3.6735(4)	5.4070(3)
c (Å)	5.028(4)	5.0328(7)	
S *z*-position	0.2559(1)	0.2602(3)	
R_w (%)	29.0		28.9
σ_Q (Å^{-1})	0.066(1)		0.033(3)
δ	0.082(9)		0.034(3)
U_{Fe} (Å^2)	0.011(8)		*U_{Ce} = 0.005(9)
U_S (Å^2)	0.012(9)		*U_O = 0.008(8)
pH	1.5		
aging	2 h at 22 °C		

[a] U = isotropic displacement parameter. (3) indicates data collected at 1-ID (energy = 80 keV). [b] Cell parameters reported by Lennie et al.[28] for a Rietveld refinement of crystalline mackinawite.

limited range of structural coherence. PDFs for the freshly precipitated samples analyzed as dry powders (FeS-A, -B, -C, and -D) and in one case as a wet slurry (FeS-E) all show a significant degree of attenuation by a distance of only ~2 nm (Figure 3a). The radial distance plotted along the abscissa was extended to emphasize the strong degree of attenuation at relatively short distance in FeS-D and FeS-F as compared to a highly crystalline CeO_2 standard (Figure 4a,b). Here, the correlations of FeS-D beyond ~2 nm terminate, reducing the signal to statistical noise and this pattern is repeated in the other fresh precipitates. Our evidence of the primary crystallite size for FeS_{fresh} from PDF analysis shows only partial agreement with prior research in which the Scherrer equation was applied to low energy XRD data and nanoscale particle sizes were calculated.[3]

It is important to note here that this attenuation in structural coherence is not due to the attenuation in the PDF that occurs at an even greater *r*-distance and is inherent to the instrument, known as the resolution dampening factor (σ_Q)[27] or instrument envelope. This envelope was evaluated independently at each beamline using highly crystalline CeO_2 with reported particle sizes >1 μm from which a refined value of σ_Q (Å^{-1}) was obtained. In all cases the refined values for CeO_2 were significantly less (i.e., exhibiting higher intensity correlations extending to a much higher radial distance) than those for both the fresh and aged precipitates examined (Tables 4 and 5). This high degree of attenuation in the PDFs for the fresh precipitates is also apparent when compared with that of highly crystalline FeS (Figure 4c). In this plot the PDF for FeS-Bulk has a comparable attenuation to that of CeO_2 collected on the same instrument. Therefore, like CeO_2, this highly crystalline sample is also representative of the instrument envelope. The range of structural coherence is the most important feature and the intensity differences evident between mackinawite and CeO_2 in Figure 4c are explained by a higher number of atom pairs at each given distance and also their corresponding scattering power. In this study, PDFs with a limited range in structural coherence have σ_Q values ranging from 0.08 to 0.15 (FeS_{fresh} and FeS_{aged}) compared to that of crystalline CeO_2 which is 0.03 at 1-ID and 0.06 at 11-IDC. Thus, from the apparent limited range of structural coherence the average primary crystallite size of the FeS_{fresh} crystallites is estimated to be on the order of ~2 nm in diameter and may be even less in certain dimensions. This finding was corroborated by direct imaging of the particles using TEM. A representative image of a freshly precipitated sample is presented (Figure 5).

Growth. Prior research[1,34] indicates that the initial FeS precipitate will develop improved long-range atomic arrangement and eventually form what is considered bulk mackinawite. It is reasonable then to hypothesize that the nanocrystalline fresh precipitates reported here will become larger upon aging through crystal growth by a mechanism such as Ostwald ripening[35] or oriented attachment.[36] An increase in the range of structural coherence in the PDF would be predicted due to growth by either mechanism. This feature was observed in the PDF for sample FeS-F (Figure 4b), which, upon aging for 1 week at 70 °C, showed correlations that clearly can be fitted by the mackinawite model to a range of ~4.5 nm. This finding was also consistent with TEM analysis and representative images of sample FeS-F are presented (Figures 6 and 7). The FeS crystallites appear to be relatively monodisperse in these two images appearing both as individual particles and as aggregates. It is difficult to say with any confidence by which mechanism(s) the particles grow.

pH Effects. The data obtained from the pH-buffered precipitates do not show significant structural changes between pH ranging from ~5 to ~8. The sample formed under the lowest pH conditions (FeS-A) had a slightly better fit as expressed in the residual difference (R_w) between the experimental PDFs and fitted model (Table 4) as compared to those samples formed at higher pH values (FeS-B, -C,

(34) Rickard, D.; Schoonen, M. A. A.; Luther, G. W. In *Geochemical Transformations of Sedimentary Sulfur*; Vairavamurthy, M. A., Schoonen, M. A. A., Eds.; American Chemical Society: Washington, DC, 1995; Vol. 612, pp 168−193.
(35) Joesten, R. L. *Rev. Mineral.* **1991**, *26*, 507−582.
(36) Penn, R. L.; Banfield, J. F. *Am. Mineral.* **1998**, *83*, 1077−1082.

Table 6. Refined Bond Lengths and Angles

Bond Lengths (Å)

	FeS-A	FeS-B	FeS-C	FeS-D	FeS-E	FeS-F	Rietveld parameters[a]
Fe−S	2.246(3)	2.248(7)	2.250(8)	2.250(3)	2.246(9)	2.254(1)	2.2558(9)
Fe−Fe	2.606(1)	2.607(3)	2.613(4)	2.612(5)	2.605(9)	2.612(8)	2.5976(3)

Bond Angles (°)

	coord. no.	FeS-A	FeS-B	FeS-C	FeS-D	FeS-E	FeS-F	Rietveld parameters[a]
S−Fe−S	2	109.09(5)	109.14(6)	109.02(6)	109.01(7)	109.11(7)	109.16(6)	109.0251
	2	110.24(6)	110.14(8)	110.38(8)	110.39(9)	110.19(8)	110.10(6)	109.6947
Fe−Fe−Fe	4	90	90	90	90	90	90	90
Fe−S−Fe	2	70.91(1)	70.86(1)	70.98(1)	70.99(2)	70.89(2)	70.84(1)	70.3053
	2	109.09(5)	109.14(6)	109.02(6)	109.01(7)	109.11(7)	109.16(6)	109.0251

[a] Bond lengths and angles reported by Lennie et al.[28] for a Rietveld refinement of crystalline mackinawite.

Table 7. Refined Bond Lengths and Angles (FeS-Bulk)

Bond Lengths (Å)

	FeS-Bulk	Rietveld parameters[a]
Fe−S	2.244(5)	2.2558(9)
Fe−Fe	2.599(8)	2.5976(3)

Bond Angle (°)

	coord. no.	FeS-Bulk	Rietveld parameters[a]
S−Fe−S	2	109.20(2)	109.0251
	2	110.02(2)	109.6947
Fe−Fe−Fe	4	90	90
Fe−S−Fe	2	70.8(3)	70.3053
	2	109.20(2)	109.0251

[a] Bond lengths and angles reported by Lennie et al.[28] for a Rietveld refinement of crystalline mackinawite.

and -D). The consistency in the derived unit cell parameters and decrease in σ_Q (Table 4) between these samples may indicate that this improvement is due primarily to a slight increase in the crystallite size of the initial precipitate under decreasing pH conditions (Figure 3a−d). This may also indicate a change in electronic structure with increasing particle size as seen in the optical properties of nanosized MoS_2 in which a change from molecule-like to solid-like band spectra was demonstrated.[37]

Aggregation. The individual FeS particles have a strong tendency to aggregate. This aggregation into larger ensembles may be one of the reasons why there has been so little consensus in the literature on the primary crystallite size and morphology of the initial FeS precipitate. Electron microscopic images presented in several studies showed poorly defined agglomerates of freshly precipitated FeS particles formed through inorganic synthesis.[3,5,38] A study of biogenic iron sulfides formed in a culture of sulfate reducing bacteria reported FeS precipitates occurring as fine-grained and platy particles on the order of 100 to 300 nm in diameter.[20] The particle sizes estimated in that study do not seem consistent with the concurrent XRD analysis in which the authors reported that the material was X-ray amorphous showing only a broad peak with a corresponding inter-planar distance of ~5 Å. Although the particle sizes reported by that study are orders of magnitude larger than the present study it is possible that the aggregation behavior of particles obscured what may also have been fundamentally a nanocrystalline material. Assembly of particles into aggregates may occur with assembly by randomly oriented stacking and may indicate localized oppositely charged regions are present on the edges versus faces of the particles. This behavior has been observed in flocculated clays and described as having edge-to-face type configurations.[39] The aggregation may also be due in part to the effects of cations while still in solution which has been shown previously to be enhanced by increasing ionic strength.[40]

Discussion

The lack of consensus between prior studies of the structure and/or crystallite size of FeS_{fresh} is primarily attributable to two factors: the extreme small size of the crystallites and their tendency to aggregate. The usefulness of more traditional techniques such as the Rietveld[41] method in refining the long-range atomic order of FeS_{fresh} have been limited by broadening of the Bragg reflections resulting primarily from submicron particle sizes.[42,43] Further, the diffuse scattering characteristic of short-range order is usually folded into the background correction in this methodology. However, the PDF method is well-suited in that it utilizes the total scattering of the sample (i.e., both the Bragg and diffuse components) and does not assume that the structure exhibits long-range periodicity.[44] A strong tendency for FeS to aggregate in solution (unpublished dynamic light scattering results) and upon processing (such as during filtering and drying) has led to a wide range of particle sizes reported in the literature. The particle sizes in a variety of studies ranged from 2 to 400 nm were reported from electron microscopic imaging (SEM and TEM), calculated from gas adsorption measurements (BET), and calculated from small-angle X-ray powder diffraction data.[3,38,45−49]

(37) Wilcoxon, J. P.; Samara, G. A. *Phys. Rev. B* **1995**, *51*, 7299−7302.
(38) Benning, L. G.; Wilkin, R. T.; Barnes, H. L. *Chem. Geol.* **2000**, *167*, 25−51.
(39) Fossum, J. O.; Gudding, E.; Fonesca, D. d. M.; Meheust, Y.; DiMasi, E.; Gog, T.; Venkataraman, C. *Energy* **2005**, *30*, 873−883.
(40) Cornwell, J. C.; Morse, J. W. *Mar. Chem.* **1987**, *22*, 193−206.
(41) Rietveld, H. M. *J. Appl. Crystallogr.* **1969**, *2*, 65−71.
(42) Scherrer, P. *Göttin Nochricht* **1918**, *2*, 98.
(43) Young, R. A. In *IUCr Monographs on Crystallography*; Young, R. A., Ed.; Oxford University Press: 1993; Vol. 5, pp 1−38.
(44) Billenge, S. J. L.; Kanatzidis, M. G. *Chem. Commun.* **2004**, *7*, 749−760.

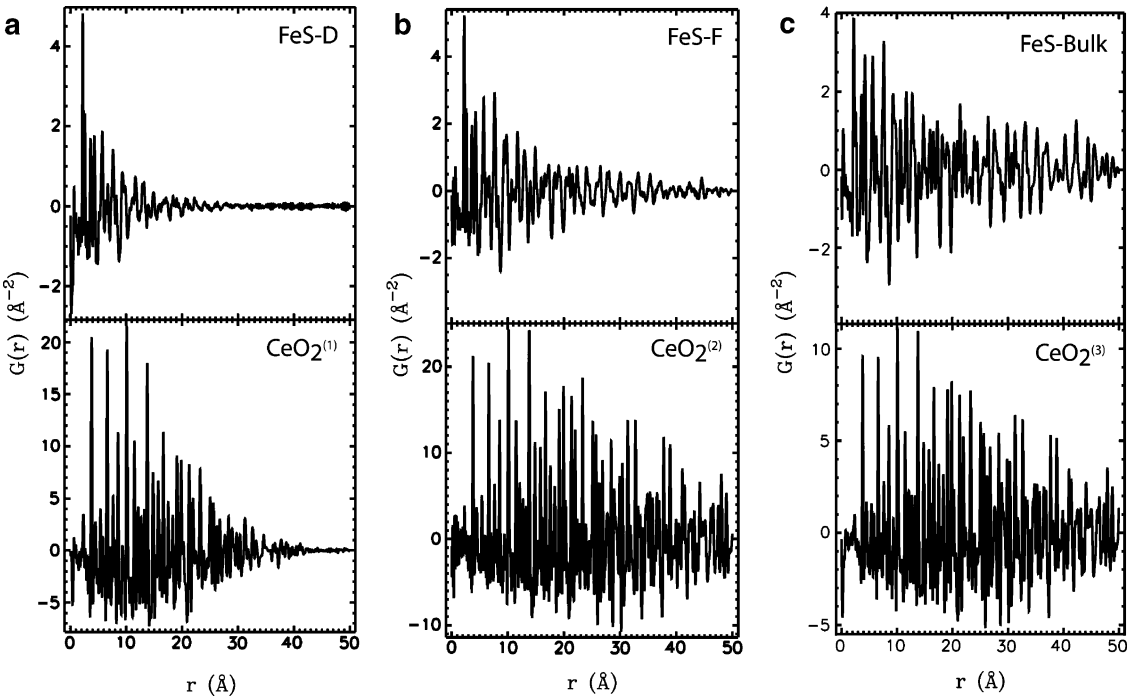

Figure 4. (a) $G(r)$ plotted out to 50 Å or 5 nm to illustrate the degree of attenuation due to the range of structural coherence, i.e., crystallite size (∼2 nm), of a sample of freshly precipitated FeS at pH 8.2. The PDF for $CeO_2^{(1)}$ is included to demonstrate the attenuation of a crystalline sample due to instrument resolution (BESSRC 11-IDC, 115 keV). Note the increased intensity and range of the correlations in the crystalline material. (b) $G(r)$ plotted out to 50 Å or 5 nm to illustrate the degree attenuation due to the range of structural coherence, i.e., crystallite size (∼4.5 nm) of a sample hydrothermally aged for one week. The PDF for $CeO_2^{(2)}$ is included to demonstrate the attenuation of a crystalline sample due to instrument resolution (1-IDC, 99.9 keV). (c) $G(r)$ plotted out to 50 Å or 5 nm to illustrate how the bulk FeS sample (FeS-Bulk) has the same attenuation as the crystalline CeO_2 standard. The PDF for $CeO_2^{(3)}$ is included to demonstrate the attenuation of a crystalline sample due to instrument resolution (1-IDC, 79.9 keV). Note again the increased intensity and range of the correlations in the crystalline material.

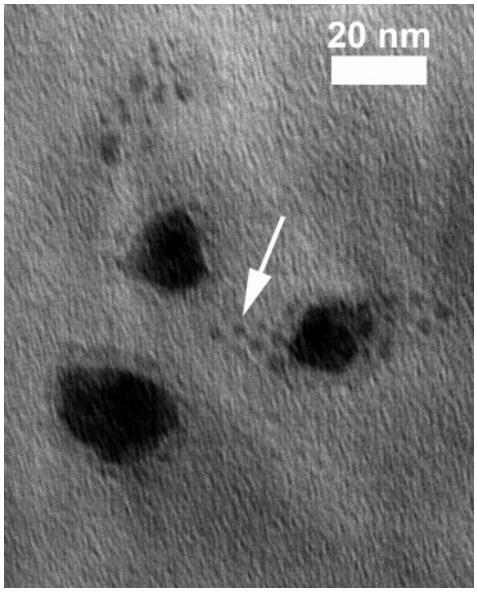

Figure 5. Transmission electron micrograph (TEM) of freshly precipitated individual FeS crystallites (arrow) approximately 2 nm in diameter and larger aggregates (260k× magnification). Scale bar indicates 20 nm.

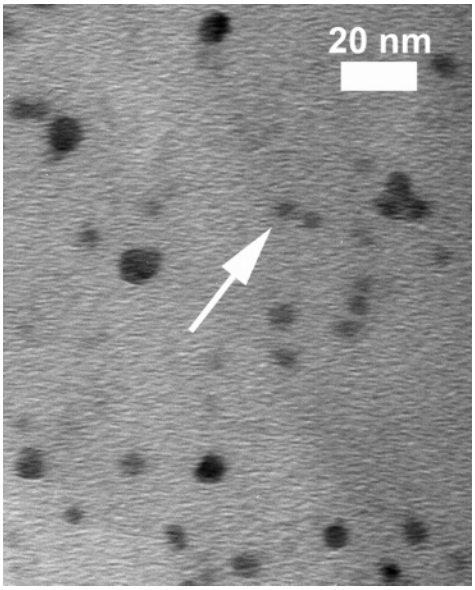

Figure 6. TEM image of FeS crystallites approximately 4−5 nm in diameter after aging (7 days at 70 °C). Slightly larger and darker particles may be aggregates of multiple smaller crystallites (260k× magnification). Scale bar indicates 20 nm.

The short- to medium-range atomic structure determined from PDF for FeS_{fresh} and FeS_{aged} are nearly identical with that of a single-phase and highly crystalline mackinawite. The short-range structure reported here is consistent with that presented in a prior investigation using X-ray absorption spectroscopy[32] and our results go further by also characterizing the medium-range structure as well as the crystallite size. Our study differs, however, from previous theories that

(45) Widler, A. M.; Seward, T. M. *Geochim. Cosmochim. Acta* **2002**, *66*, 383−402.
(46) Rickard, D.; Luther, G. W. *Geochim. Cosmochim. Acta* **1997**, *61*, 135−148.
(47) Rickard, D. T. *Am. J. Sci.* **1975**, *275*, 636−652.
(48) Kornicker, W. A. Interactions of divalent cations with pyrite and mackinawite in seawater and sodium-chloride solutions. Ph.D. Thesis, Texas A&M University, 1988.
(49) Taylor, P.; Rummery, T. E.; Owen, D. G. *J. Inorg. Nucl. Chem.* **1979**, *41*, 1683−1687.

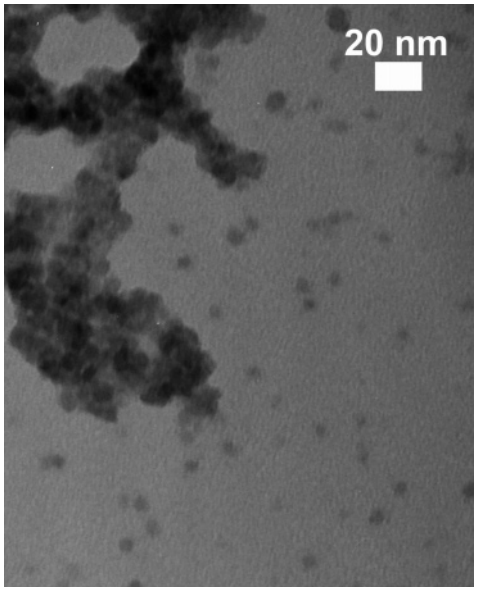

Figure 7. TEM image of FeS crystallites after aging (7 days at 70 °C). Individual particles appear relatively monodisperse and are also apparent in larger aggregates (160k× magnification). Scale bar indicates 20 nm.

have described the initial precipitate as either a mixture of mackinawite and greigite (Fe_3S_4)[15] or as a mixture of two end-member mackinawite phases (MkA and MkB) each with distinct long-range ordering.[3,50] The former hypothesis, proposed nearly 40 years ago, was based on observations of XRD data collected using low-energy Cu radiation. The presence of greigite as a secondary phase was difficult to discern with any certainty since the scatter from the initial FeS precipitate was weak overall with broadened peaks. In the XRD pattern presented the peak positions suggested only the presence of poorly crystalline material with a mackinawite-like structure. In the present study, greigite was not observed in any of the nanocrystalline FeS samples (FeS_{fresh} and FeS_{aged}) formed by the commonly used rapid-mixing method. Although greigite was detected in FeS-Bulk as a secondary phase we believe this to be the result of oxidized iron impurities in the iron wool used in the synthesis. To illustrate how the PDFs for other iron sulfide phases would differ from that of mackinawite a series of patterns have been calculated using PDFFit (Figure 8). It is clear that the interatomic distances for mackinawite are distinct from those of other iron sulfide phases (e.g., greigite, smythite, pyrrhotite, and troilite) and therefore these would not provide an adequate fit to the experimental data presented here.

In the latter and more recent study, Wolthers et al.[50] presented a model of the initial FeS precipitate to explain their scattering results collected using a low-energy X-ray source. The model consisted of a disordered mixture of two mackinawite phases (30% MkA and 70% MkB) with the proportion of the minor phase (MkA) decreasing with aging. Two distinct primary crystallite sizes of 2.2 × 1.7 nm and 7.4 × 2.9 nm were calculated for MkA and MkB, respectively, using the Scherrer equation. Although TEM data were presented there were no images of individual crystallites to confirm the sizes calculated from XRD. The difficulties

(50) Wolthers, M.; Van der Gaast, S. J.; Rickard, D. *Am. Mineral.* **2003**, *88*, 2007−2015.

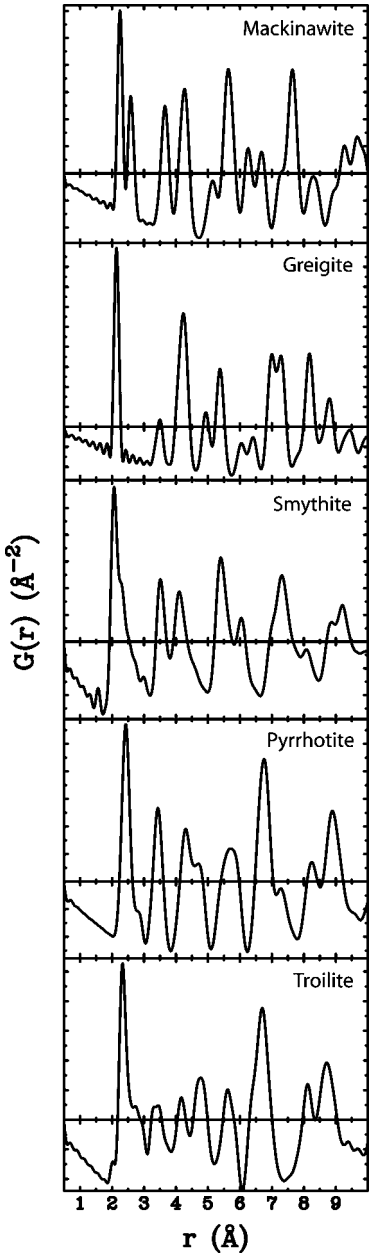

Figure 8. Calculated $G(r)$ for several iron sulfide phases including mackinawite (FeS), greigite (Fe_3S_4), smythite (Fe_3S_4), pyrrhotite (~Fe_7S_8), and troilite (FeS).

encountered in the application of peak-width-based analysis to nanocrystalline materials have been pointed out by Hall et al.[12] We believe that use of the Scherrer equation is questionable given the limited quality of data obtainable using a low-energy X-ray source. However, it is interesting that the size reported for the minor phase (MkA) is approximately the same as the size reported in the present study. The unit cell parameters reported (MkA: $a = 4.0$ Å, $c = 6.7 \pm 0.1$ Å) and (MkB: $a = 3.7$ Å, $c = 5.5 \pm 0.2$ Å) would indicate that a relatively large relaxation of the atomic structure occurred and resulted in the distance separating the basal planes to increase as much as 33% from that of crystalline FeS. This proposed lattice expansion was explained by the effects of intercalated water molecules and small crystallite size. It was also used in part to explain the high adsorptive capacity of the initial FeS precipitate for divalent metals also noted in previous studies.[48,51−53] In the

present study we find that no significant relaxation is observed in the structure of FeS_{fresh} and FeS_{aged} as represented in the refined unit cell parameters derived from PDF analysis. Further, the initial precipitate formed is both single-phase and nanocrystalline mackinawite even under varying pH conditions.

Conclusions

Amorphous, or X-ray amorphous, is a common term used in the geo- and marine sciences communities to describe mineral precipitates lacking long-range order. The initial FeS precipitate has long been described in this way primarily from observations made using traditional XRD techniques. An amorphous solid by definition refers to a material in which the positions of atoms are lacking long-range order. On short-range scales ($< \sim 1$ nm), however, amorphous solids typically do exhibit order. It is difficult to make the distinction between materials that are truly amorphous and solids in which the size of the crystallites are extremely small. Electron imaging and traditional XRD techniques may have difficulty in distinguishing between amorphous and crystalline structures on these length scales. The relatively recent application of high-energy XRD and PDF analysis to nanocrystalline solids provides a new tool for adequately characterizing and understanding such materials. This study shows that the initial FeS precipitate is in fact highly ordered over short- and medium-range atomic scales even with such extremely small crystallites. Hence, the initial FeS precipitate is better described as a nanocrystalline material with mackinawite structure. Work in progress exploring pH effects on particle size, growth mechanisms, growth rate and morphology using time-resolved method experiments and reverse Monte Carlo simulations will be included in upcoming communications.

Acknowledgment. This work is funded by the Center for Environmental Molecular Science (CEMS) through the National Science Foundation (Award CHE-0221934). Data collection was performed at the Basic Energy Sciences Synchrotron Research Center (BESSRC-CAT) 11-IDC and XOR 1-ID at the Advanced Photon Source, Argonne National Laboratory. Use of the Advanced Photon Source was supported by the U.S. Department of Energy, Office of Science, Office of Basic Energy Sciences, under Contract W-31-109-Eng-38. The authors are grateful for the thoughtful insight and technical support provided by Dr. James Quinn.

CM050886B

(51) Morse, J. W.; Arakaki, T. *Geochim. Cosmochim. Acta* **1993**, *57*, 3635−3640.
(52) Arakaki, T.; Morse, J. W. *Geochim. Cosmochim. Acta* **1993**, *57*, 9−14.
(53) Wharton, M. J.; Atkins, B.; Charnock, J. M.; Livens, F. R.; Pattrick, R. A. D.; Collison, D. *Appl. Geochem.* **2000**, *15*, 347−354.